NASA
Technical
Paper
2600

August 1986

Cross Section Calculations for Subthreshold Pion Production in Peripheral Heavy-Ion Collisions

John W. Norbury,
Francis A. Cucinotta,
Philip A. Deutchman,
and Lawrence W. Townsend

NASA

NASA Technical Paper 2600

1986

Cross Section Calculations for Subthreshold Pion Production in Peripheral Heavy-Ion Collisions

John W. Norbury and
Francis A. Cucinotta
Old Dominion University
Norfolk, Virginia

Philip A. Deutchman
University of Idaho
Moscow, Idaho

Lawrence W. Townsend
Langley Research Center
Hampton, Virginia

National Aeronautics
and Space Administration

**Scientific and Technical
Information Branch**

Introduction

In individual nucleon-nucleon collisions, pion production at energies lower than 290 MeV is forbidden by energy conservation. However, in nucleus-nucleus collisions, pions have been produced at energies as low as 25 MeV/nucleon (refs. 1 and 2), far below the nucleon-nucleon threshold. Such subthreshold meson production is one of the most fascinating phenomena to be observed in heavy-ion collisions in recent years. One of the original suggestions that such pions might be observed dates back to McMillan and Teller (ref. 3), who hypothesized that nucleons could be boosted to energies above threshold by their Fermi motions within the nucleus. The first theoretical model of this type, developed by Bertsch (ref. 4), has been applied to various sets of experimental data (refs. 5 and 6). Since the pions in this model are produced by a nucleon-nucleon single collision (NNSC) process whose probability decreases with increasing boosts, it is insufficient to adequately explain all the data (refs. 6 and 7). However, the possibility that some of the inclusive pion data are the result of this process is not ruled out, since it is likely that several competing processes may contribute, especially for incident energies well above the absolute threshold.

Since NNSC models are unable to explain all the data, statistical and thermal models have been proposed (refs. 6 and 8–10). In these models, the pions are produced by statistical processes, and the associated production cross sections are determined from the phase space available to them. The two major variations in this approach involve either (1) compound nucleus decay (ref. 9) in which pions and nucleons boil off after statistical equilibrium is achieved among the nucleons in the entire nucleus or (2) statistical equilibrium and subsequent evaporation within subgroups of nucleons (ref. 10) (i.e., "hot spots") or composite fragments (refs. 6 and 8). At the absolute nucleus-nucleus threshold, pionic fusion, also termed doubly coherent production, may be the only possible mechanism for pion production. In this process, the colliding nuclei fuse to form a compound system and an emitted pion (refs. 11–13). Examples of this mechanism include the reactions $^{3}\mathrm{He}(^{6}\mathrm{Li},\pi^{-})^{9}\mathrm{C}$ and $^{3}\mathrm{He}(^{3}\mathrm{He},\pi^{+})^{6}\mathrm{Li}$ discussed in references 11 and 12, respectively.

Apart from NNSC and statistical or thermal models, the third grouping into which the theoretical models may be classified (ref. 14) is the collective models. The two main categories here are pionic bremsstrahlung (refs. 15–17) and models based on the Weizsäcker-Williams method (refs. 18–27) originally used in electrodynamics (ref. 28). This latter method was originally used to describe nuclear fragmentation (ref. 29) and has since been extended and utilized to describe pion production by Hiller and Pirner (refs. 18 and 19) and by Brown, Deutchman, Townsend, Madigan, Norbury, and Cucinotta (refs. 20–27). In its latest formulation (refs. 26 and 27) (described in the next section), which forms the basis of the calculations in the present paper, it will be referred to as the "particle-hole model."

Description and History of Particle-Hole Model

We begin by briefly describing the "particle-hole model" as used in the present calculations. Modifications to the previous formulation (ref. 26) and a brief account of its historical development are also presented. Then, total cross sections, angular distributions, spectral distributions, doubly differential cross sections, and Lorentz-invariant differential cross sections for neutral and charged pions produced in carbon-carbon collisions in the energy range of 35 to 86 MeV/N are calculated and compared with recent heavy-ion pion data. Finally, the effects on the cross sections of including Pauli blocking and pion absorption are investigated.

Pions can be produced by means of intermediate isobar $\Delta(3,3)$ formation in both $\pi N \rightarrow \Delta \rightarrow \pi N$ and $NN \rightarrow N\Delta \rightarrow NN\pi$ processes. In the former process, a real pion interacts with a nucleon to form an isobar which subsequently decays back to a pion and nucleon. The latter process is similar to the former except that the real incident pions are replaced by virtual incident pions with the incident nucleon acting as the source for the virtual pions. Hence, the second reaction proceeds in the same manner as the first, except that the incident pions are virtual rather than real.

It is important to realize that the virtual pion cloud surrounding a nucleus can be quite different from the virtual pion cloud surrounding a nucleon (refs. 18–20). This difference is essential to the present description (refs. 20–27) of subthreshold pion production. It is the nucleus as a whole which determines the properties of the virtual pion cloud (in particular, its energy spectrum). In this description, these *nuclear* virtual pions impinge on the nucleons in the other nucleus to form isobars which subsequently decay into real pions.

This model was first proposed by Brown and Deutchman (ref. 20), who were interested not only in subthreshold pion production but also in a corresponding signature unique to the above reaction mechanism, since it was realized that neither this mechanism (nor perhaps any other) would explain all the inclusive cross section data. Implicit in the

above description is the notion of a grazing or peripheral (as opposed to central) collision. If the isobar forms in the projectile nucleus, then the target will go to an excited state because of conservation of spin and isospin. Various states are possible, but the ones concentrated on are the isovector triplet including the magnetic dipole (M1) giant resonance in ^{12}C, since it decays by emission of a 15.11-MeV photon in coincidence with the escaping pion, which comes from the decay of an isobar in an ^{16}O projectile nucleus and thus gives a unique signature to the above reaction mechanism.

The above ideas were the basis for a first-quantized formalism (refs. 21–25). Later, however, the whole theory was reformulated in second quantization in which the simultaneous excitation of an M1 giant resonance and a $\Delta(3,3)$ giant resonance was described in a particle-hole model (refs. 26 and 27).

Present Developments

The main purpose of a previous paper by Norbury, Deutchman, and Townsend (ref. 26) was to present the basic particle-hole model. In it, Lorentz-invariant and doubly differential cross sections for ^{16}O incident upon ^{12}C at 2.1 GeV/N and 85 MeV/N at single fixed angles were presented. In the present work, we have evaluated cross sections for ^{12}C incident upon ^{12}C because of the greater availability of experimental data for this reaction. Consequently the $1p_{1/2}$ shell is no longer filled with nucleons, so the particle-hole coefficients $\chi_{ph}(P)$ describing the probability for excitation of a particular nucleon to an isobar are different from previous work, as are the sums over various j values. The net result is that the Lorentz-invariant differential cross section for pion production in a ^{12}C projectile with M1 giant resonance formation in a ^{12}C target now becomes (ref. 26)

$$\frac{d^3\sigma\left(\pi_{T_f}\right)}{c^3\, d^3p_\pi/E_\pi} = \frac{16}{13}\frac{27}{25}\frac{2}{\pi^2}\left(\frac{4}{3}\right)^5 f^2\left(\frac{p_\beta c}{m_\pi c^2}\right)^2 \times \frac{\sigma_{\Delta T}(\omega_\Delta)}{\left(T_N + T_\pi + m_\pi c^2 + m_N c^2 - m_\Delta c^2\right)^2 + (\Gamma_\Delta/2)^2} \times F^2\left(\mathbf{k}_{\beta_\pi}\right)\, f^2\left(\mathbf{k}_{\beta_\pi}\right) \tag{1}$$

where $\sigma_{\Delta T}(\omega_\Delta)$, the isobar formation cross section, is given by equation (64) in reference 26, and the form factors $F^2\left(\mathbf{k}_{\beta_\pi}\right)$ and $f^2\left(\mathbf{k}_{\beta_\pi}\right)$ are given by equations (39) and (48) in that same work. The unrationalized coupling constant, $f^2 = 0.08$, and the other symbols, if not obvious, are described in reference 26. Note that nucleon recoil is now included in the Breit-Wigner term by the explicit dependence on the nucleon kinetic energy T_N.

In previous work (refs. 20–26), the $\Delta(3,3)$ formation in the projectile with M1 formation in the target was considered. In the present work, we have also summed contributions from the process in which the $\Delta(3,3)$ forms in the target with M1 formation in the projectile. Summing these contributions is important, as there is no way for experimentalists to distinguish between the pions from the projectile or the target. In the present work, we have also performed extensive numerical integrations, so that angular ($d\sigma/d\Omega$), spectral ($d\sigma/dE$), and total cross sections can be calculated in various reference frames. Furthermore, the presentation of cross sections for a much larger range of projectile subthreshold energies and pion angles allows a much wider comparison with experimental data. The effects of Pauli blocking and pion absorption are studied by varying the width Γ_Δ of the isobar resonance (refs. 18 and 30) according to the prescription of Hiller and Pirner (ref. 18) where

$$\Gamma_\Delta = \lambda\Gamma_{\text{free}} + \Gamma_{\text{abs}} \tag{2}$$

with Γ_{free} representing the free width of the isobar (115 MeV). The fraction λ accounts for Pauli blocking as the free width is reduced as a result of the closed decay channels when the Δ is a nuclear medium. The term Γ_{abs} accounts for pion absorption effects.

The final improvement is that we now distinguish between charged and neutral pions from considerations of pions produced in elementary nucleon-nucleon collisions by means of isobar formation (refs. 31 and 32). Here one simply calculates the probabilities (i.e., isotopic spin Clebsch-Gordon coefficients) of pion production through the various possible channels and then deduces the relative contributions of the proton-proton (pp), proton-neutron (pn), or neutron-neutron (nn) cross sections for producing a particular pion species. The contribution (refs. 31 and 32) for π^0 production is

$$1/3\sigma_{pp} + 2/3\sigma_{pn}$$

and the contribution for π^+ or π^- production is

$$5/6\sigma_{pp} + 1/6\sigma_{pn}$$

with the assumption that

$$\sigma_{pp} = \sigma_{nn} \tag{3}$$

Note that the cross section for π^+ and π^- production is the same in the above simple picture.

Results

Neutral Pion Production

Since the results displayed in this work represent the sum of cross sections for pions being produced either in the projectile or in the target (unless otherwise indicated), it is instructive to decompose the summed Lorentz-invariant differential cross section into the projectile and target contributions. This is done in figure 1 for neutral pions produced at 0° in the laboratory by 75 MeV/N carbon-carbon collisions. As expected, in the laboratory frame low-energy pions are produced mainly from the target, whereas the higher energy pions come from the projectile. The dip in the projectile cross section curve at about 10 MeV is caused by the fact that the cross section is zero for pions of zero energy in the rest frame of the nucleus emitting them. The net effect of summing projectile and target cross sections is a broader energy distribution than that obtained from consideration of pions produced only from the projectile nucleus (ref. 26). In figure 2, the Lorentz-invariant neutral pion production cross sections for 75 MeV/N carbon-carbon scattering are presented as a function of laboratory pion kinetic energy and angle. As expected, the cross section decreases at higher pion energies as the laboratory angle increases. Similar behavior is displayed in figure 3 for the noninvariant doubly differential cross section at 85 MeV/N.

As mentioned previously, the present work studies pion production in the carbon-carbon collision system, rather than the oxygen-carbon system of reference 26, so that more definitive comparisons with recent experimental data are made. Figure 4 presents spectral distributions for various subthreshold projectile energies. Also plotted are the experimental measurements of Noll et al. (ref. 7). Since we have no arbitrarily adjusted parameters or scale factors in our theory, the quantitative agreement between theory and experiment is excellent. Discrepancies between theory and experiment are largely the result of the inclusive nature of the experimental data, whereas the theory represents an exclusive process. One would therefore expect that the agreement between the inclusive data and the exclusive theory should improve as the projectile energy is lowered (ref. 24), and this is clearly true for these spectral distributions. This improving agreement is also obvious in the total cross sections displayed in figure 5. Agreement with the total cross section at 35 MeV/N is within the quoted error. Thus one would expect that the prediction of the spectral distribution at 35 MeV/N (in fig. 4) would reproduce the full inclusive spectrum at this energy. We encourage experimentalists to undertake such measurements in order to test this prediction.

Although not plotted, the π^0 total production cross section at 25 MeV/N for $^{16}O + {}^{27}Al$ is estimated to be 5.0 nb by using the "scaling" formula (ref. 33)

$$\sigma(\mathrm{O-Al}) = \left(\frac{27 \times 16}{12 \times 12}\right)^{2/3} \sigma(\mathrm{C-C}) \qquad (4)$$

This calculated value compares very well with the recently measured value (ref. 2) of 5.8 nb. (Note that one must be very careful in using eq. (4) for incident energies close to absolute threshold.) However, because the theoretical value quoted above does not include threshold effects, the above scaling formula should be approximately valid.

For the sake of further qualitative comparisons of the shape of the spectral and angular distributions, the inclusive data of Braun-Munzinger et al. (ref. 1) are presented for the reaction $\mathrm{Al}(^{14}\mathrm{N}, \pi^0)$ in figures 6 and 7. Also shown are calculated values for the carbon-carbon system. Although the nuclei are different and only rough qualitative agreement is sought, one can see that the magnitudes and shapes are reasonably well predicted by our theory. Again measurements for the carbon-carbon system would be helpful to validate the theory.

In summary, the agreement between theory and experiment is quantitatively excellent for the production of neutral pions especially in view of the lack of any arbitrarily adjusted parameters in the theoretical formalism.

Charged Pion Production

The Lorentz-invariant differential cross sections for π^+ production at 85 and 75 MeV/N are shown in figures 8 and 9 together with the data of Bernard et al. (ref. 34), and Johansson et al. (ref. 5). Noninvariant doubly differential cross sections at 85 MeV/N are shown in figure 10 with the data of Johansson et al. (ref. 5) and Jakobsson (ref. 35). For the higher pion energies, the qualitative behavior of the theoretical predictions follows the data in that there is a decrease in the cross sections as the pion energy is increased and also as the angle increases. However, the quantitative agreement between theory and experiment for the charged pions is not as good as the agreement for neutral pions.

By comparing our theoretical predictions for π^+ production in figures 9 and 10 with those for π^0 production in figures 2 and 3, one can see that the cross sections are quite similar. As noted before, comparison between theory and experiment for π^0 production is very good. Thus we attribute the poorer agreement for π^+ production to the fact that we have not included Coulomb distortion effects (refs. 36–38).

It is well known, for instance, that the π^+/π^- ratio varies significantly (refs. 36–38), yet at present, this ratio is always unity in theory. Work on Coulomb effects is currently underway and is considered to be of crucial importance in applying our theory to charged pion data.

The curves for $\Theta_\pi = 90°$ in figure 10 are shown again in figure 11, but this time a decomposition of the summed cross section is shown for charged pions coming from the projectile and target at 90°. At this angle, the behavior is reversed from that in figure 1. At 90°, the higher energy pions observed in the laboratory come mainly from the target, whereas lower energy pions come from the projectile. Continuing with comparison to the charged pion data, figure 12 shows noninvariant cross section data of Chiavassa et al. (ref. 39) for both π^+ and π^- at 0°. Clearly the π^+/π^- ratio varies significantly. Shown also are our calculated values for charged pions.

Figures 13 and 14 show angular distributions in which the exclusive theoretical results are below the inclusive data at 85 MeV/N. These results are consistent with the results from the spectral and total cross sections for π^0 production (figs. 4 and 5) at 84 MeV/N. Since the calculation is exclusive, exact agreement is not expected at energies as high as 85 MeV/N. (Recall that the agreement for π^0 production improved substantially for lower projectile energies.) These angular distribution results are also consistent with the kinetic energy distribution comparisons of figures 8–12. There the experimental data were generally well above the theoretical predictions (again at the higher projectile energies). The angular distributions involve an integration over pion kinetic energy, and thus if the kinetic energy distributions are mostly below the data, one would expect the same to be true of the angular distributions. Note in figure 14 that even though the calculated values are well below the experimental data, the qualitative behavior observed experimentally of cross sections falling as the pion energy increases is predicted theoretically as well.

Summarizing the results for charged pion production, we see in general that the theoretically predicted values are lower than the experimentally observed data at 75 to 86 MeV/N, a result consistent with the neutral pion results. Further work on including Coulomb distortion effects is clearly important and needed for definitive comparisons with the data.

Pauli Blocking and Pion Absorption

In this section we make a very preliminary investigation of Pauli blocking and pion absorption effects by noting that all the calculations presented so far have made use of a free isobar width of 115 MeV. If a nucleon is excited to an isobar in a certain shell model state, then it becomes possible for a nucleon in a higher state to fill the nucleon hole that was created below it before the isobar decays. Therefore when the isobar does eventually decay into a nucleon and pion, there is now no vacant hole for the nucleon to fall into. Thus the decay of the isobar is inhibited, which means that the half-life of an isobar in a nuclear medium will be longer than its free half-life. Consequently, the decay width of an isobar in a nuclear medium is smaller than that of a free isobar. This effect is represented by the $\lambda\Gamma_{\text{free}}$ term in equation (2), where λ is a fraction less than unity, and $\lambda\Gamma_{\text{free}}$ represents the nuclear decay width due to Pauli blocking. There is, however, another effect that tends to increase the width. Not only can the isobar have interactions within the nuclear medium (refs. 40 and 41), but after the isobar decays, the emitted pions can be absorbed in the nuclear medium (refs. 42–44). This effect is known to be dependent on the pion energy (refs. 42–44). These subsequent interactions of the pions lead to an effective increase of the isobar decay width (ref. 14).

We follow the work of Hiller and Pirner (ref. 18) and take the width due to Pauli blocking to be about 80 MeV (with $\lambda \approx 0.7$) and the pion absorption width to be 120 MeV. Thus the width with both Pauli blocking and pion absorption is about 200 MeV (ref. 18). In figures 15 through 19, graphs for an isobar width of 115 MeV (from figs. 4, 6, 7, 8, and 12) are presented with graphs for isobar widths of 80 and 200 MeV. In figures 16 through 19, as the width increases, the cross section decreases as expected, since larger widths effectively correspond to greater pion absorption and thus reduce the pion production cross section. It is noted, however, that the cross sections are not drastically modified by Pauli blocking and pion absorption effects but vary at most by an approximate factor of 2 when changing the width from 80 to 200 MeV. Again, this approach represents only a preliminary study of these effects. In a more sophisticated treatment, the pion absorption should really be made dependent on the pion energy and the charge species, and these effects may introduce some anisotropy into the angular correlations.

Concluding Remarks

A particle-hole calculation for subthreshold pion production by means of intermediate isobar and magnetic dipole (M1) giant resonance formation has been extended to a study of the carbon-carbon system. The modifications and improvements to the theory include a ^{12}C projectile (rather than ^{16}O), nucleon recoil, summation of pions from both projectile and

target (rather than projectile only), calculations of spectral, angular, and total cross sections in various reference frames (by numerical integrations), an increased range of subthreshold projectile energies, considerations of Pauli blocking and pion absorption, and the distinction between neutral and charged pion species. Extensive comparisons with experimental data have been made, and excellent agreement has been achieved for neutral pions. Disparities for charged pions illustrate the need to include Coulomb distortion.

NASA Langley Research Center
Hampton, VA 23665-5225
June 2, 1986

References

1. Braun-Munzinger, P.; Paul, P.; Ricken, L.; Stachel, J.; Zhang, P. H.; Young, G. R.; Obenshain, F. E.; and Grosse, E.: Pion Production in Heavy-Ion Collisions at E_{lab}/A = 35 MeV. *Phys. Rev. Lett.*, vol. 52, no. 4, Jan. 23, 1984, pp. 255–258.
2. Obenshain, F. E.; Plasil, F.; Young, G. R.; Braun-Munzinger, P.; Freifelder, R.; and Stachel, J.: Measurement of Neutral Pion Production Cross Section for $^{16}O + {}^{27}Al$ at 25 MeV/Nucleon. *Bull. American Phys. Soc.*, vol. 30, no. 4, Apr. 1985, p. 768.
3. McMillan, W. G.; and Teller, E.: On the Production of Mesotrons by Nuclear Bombardment. *Phys. Rev.*, Second ser., vol. 72, no. 1, July 1, 1947, pp. 1–6.
4. Bertsch, G. F.: Threshold Pion Production in Heavy-Ion Collisions. *Phys. Rev. C.*, Third ser., vol. 15, no. 2, Feb. 1977, pp. 713–718.
5. Johansson, T.; Gustafsson, H.-Å.; et al.: Subthreshold Pion Production in Heavy-Ion Collisions at 85A MeV. *Phys. Rev. Lett.*, vol. 48, no. 11, Mar. 15, 1982, pp. 732–735.
6. Shyam, R.; and Knoll, J.: Subthreshold Pion Production in Nucleus Collisions—A Cooperative Process! *Phys. Lett.*, vol. 136B, no. 4, Mar. 8, 1984, pp. 221–225.
7. Noll, H.; Grosse, E.; Braun-Munzinger, P.; Dabrowski, H.; Heckwolf, H.; Klepper, O.; Michel, C.; Müller, W. F. J.; Stelzer, H.; Brendel, C.; and Rösch, W.: Cooperative Effects Observed in the π^0 Production From Nucleus-Nucleus Collisons. *Phys. Rev. Lett.*, vol. 52, no. 15, Apr. 9, 1984, pp. 1284–1287.
8. Shyam, R.; and Knoll, J.: A Cooperative Mechanism of Subthreshold Pion Production. *Nucl. Phys.*, vol. A426, no. 3, Sept. 24, 1984, pp. 606–624.
9. Aichelin, J.; and Bertsch, G.: Subthreshold Pions From the Compound Nucleus? *Phys. Lett.*, vol. 138B, no. 5, 6, Apr. 26, 1984, pp. 350–352.
10. Aichelin, J.: New Evidence for "Hot Spots" From Subthreshold Pions. *Phys. Rev. Lett.*, vol. 52, no. 26, June 25, 1984, pp. 2340–2343.
11. Aslanides, E.; Fassnacht, P.; Hibou, F.; Chiavassa, E.; Dellacasa, G.; Gallio, M.; Musso, A.; Bressani, T.; and Puddu, G.: Doubly Coherent Production of π^- by ^{3}He Ions of 910 MeV. *Phys. Rev. Lett.*, vol. 43, no. 20, Nov. 12, 1979, pp. 1466–1470.
12. Germond, Jean-François; and Wilkin, Colin: Coherent Pion Production in ^{3}He-^{3}He Collisions. *Phys. Lett.*, vol. 106B, no. 6, Nov. 26, 1981, pp. 449–452.
13. Le Bornec, Y.; Bimbot, L.; Koori, N.; Reide, F.; Willis, A.; Willis, N.; and Wilkin, C.: Coherent Pion Production Near Threshold With a ^{3}He Projectile. *Phys. Rev. Lett.*, vol. 47, no. 26, Dec. 28, 1981, pp. 1870–1874.
14. Guet, C.; and Prakash, M.: Knock Out for Subthreshold Pion Production. *Nucl. Phys.*, vol. A428, Oct. 22, 1984, pp. 119c–135c.
15. Vasak, David; Stöcker, Horst; Müller, Berndt; and Greiner, Walter: Pion Bremsstrahlung and Critical Phenomena in Relativistic Nuclear Collisions. *Phys. Lett.*, vol. 93B, no. 3, June 16, 1980, pp. 243–246.
16. Vasak, D.; Müller, B.; and Greiner, W.: Pion Radiation From Fast Heavy Ions. *Phys. Scr.*, vol. 22, 1980, pp. 25–35.
17. Vasak, David; Greiner, Walter; Müller, Berndt; Stahl, Thomas; and Uhlig, Mark: Pionic Bremsstrahlung in Heavy-Ion Collisions. *Nucl. Phys.*, vol. A428, Oct. 22, 1984, pp. 291c–303c.
18. Hiller, Brigitte; and Pirner, Hans J.: Coherent π^- Production in $He^3 + Li^6 \rightarrow \pi^- + X$ at 303 MeV/N. *Phys. Lett.*, vol. 109B, no. 5, Mar. 4, 1982, pp. 338–340.
19. Pirner, Hans J.: Quasiparticle Properties of the Pion and Heavy-Ion Collisions. *Phys. Rev. C*, Third ser., vol. 22, no. 5, Nov. 1980, pp. 1962–1970.
20. Brown, G. E.; and Deutchman, P. A.: Coherent Pion Production in 100 MeV/A C^{12}-Heavy Target Scattering With High Resolution. Paper presented at Workshop on High Resolution Heavy Ion Physics (Saclay, France), May 31–June 2, 1978.
21. Townsend, L. W.; and Deutchman, P. A.: Isobar Giant Resonance Formation in Self-Conjugate Nuclei. *Nucl. Phys.*, vol. A355, 1981, pp. 505–532.
22. Deutchman, P. A.; and Townsend, L. W.: Coherent Isobar Production in Peripheral Relativistic Heavy-Ion Collisions. *Phys. Rev. Lett.*, vol. 45, no. 20, Nov. 17, 1980, pp. 1622–1625.
23. Deutchman, P. A.; and Townsend, L. W.: Isobars and Isobaric Analog States. *Phys. Rev.*, ser. C, vol. 25, no. 2, Feb. 1982, pp. 1105–1107.
24. Townsend, L. W.; Deutchman, P. A.; Madigan, R. L.; and Norbury, J. W.: Pion Production Via Isobar Giant Resonance Formation and Decay. *Nucl. Phys. A*, vol. 415, Mar. 19, 1984, pp. 520–529.
25. Deutchman, P. A.; Madigan, R. L.; Norbury, J. W.; and Townsend, L. W.: Pion Production Through Coherent Isobar Formation in Heavy-Ion Collisions. *Phys. Lett.*, ser. B, vol. 132, no. 1, 2, 3, Nov. 24, 1983, pp. 44–46.
26. Norbury, J. W.; Deutchman, P. A.; and Townsend, L. W.: A Particle-Hole Calculation for Pion Production in Relativistic Heavy-Ion Collisions. *Nucl. Phys. A*, vol. 433, no. 4, Feb. 18, 1985, pp. 691–712.
27. Norbury, J. W.; Cucinotta, F. A.; Deutchman, P. A.; and Townsend, L. W.: Theoretical Spectral Distributions and Total Cross Sections for Neutral

Subthreshold Pion Production in Carbon-Carbon Collisions. *Phys. Rev. Lett.*, vol. 55, no. 7, Aug. 12, 1985, pp. 681–683.

28. Jackson, John David: *Classical Electrodynamics,* Second ed. John Wiley & Sons, Inc., c.1975.
29. Feshbach, Herman; and Zabek, Mark: Fragmentation of Relativistic Heavy Ions. *Ann. Phys.*, vol. 107, nos. 1–2, Sept. 6, 1977, pp. 110–125.
30. Dillig, M.; and Huber, M. G.: Is There a Giant (3,3) Resonance in Nuclei? *Phys. Lett.*, vol. 48B, no. 5, Mar. 4, 1974, pp. 417–419.
31. Lock, W. O.; and Measday, D. F.: *Intermediate Energy Nuclear Physics.* Methuen & Co. Ltd., 1970, p. 220.
32. Pilkuhn, Hartmut M.: *Relativistic Particle Physics.* Springer-Verlag, c.1979, p. 404.
33. Stachel, J.: Pion Production in Heavy Ion Collisions Close to Absolute Thresholds. Paper presented at the 7th High Energy Heavy Ion Study, GSI, Darmstadt (Federal Republic of Germany), Oct. 1984.
34. Bernard, V.; Girard, J.; et al.: Production of Charged Pions in Intermediate-Energy Heavy-Ion Collisions. *Nucl. Phys.*, vol. A423, no. 3, July 23, 1984, pp. 511–524.
35. Jakobsson, B.: Pions Produced in Heavy Reactions Far Below the Free Nucleon-Nucleon Scattering Threshold. *Phys. Scr.*, vol. T5, 1983, pp. 207–212.
36. Benenson, W.; Bertsch, G.; et al.: Low-Energy Pion Production at 0° With Heavy Ions From 125 to 400 MeV/Nucleon. *Phys. Rev. Lett.*, vol. 43, no. 10, Sept. 3, 1979, pp. 683–686; Errata, vol. 44, no. 1, Jan. 7, 1980, p. 54.
37. Bertsch, G.: Charge Dependence of Pion Production in Heavy Ion Collisions. *Nature,* vol. 283, no. 5744, Jan. 17, 1980, pp. 280–281.
38. Gyulassy, M.; and Kauffmann, S. K.: Coulomb Effects in Relativistic Nuclear Collisions. *Nucl. Phys.*, vol. A362, no. 2, June 8, 1981, pp. 503–533.
39. Chiavassa, E.; Costa, S.; et al.: Pion Production in ^{12}C-Nucleus Interactions at 86 MeV/Nucleon. *Nucl. Phys.*, vol. A422, no. 3, July 2, 1984, p. 621–634.
40. Ginocchio, J. N.: Deep Inelastic Pion-Induced Nuclear Reactions in the Isobar Model. *Phys. Rev. C,* Third ser., vol. 17, no. 1, Jan. 1978, pp. 195–214.
41. Moniz, E. J.: Δ-Nucleus Interactions. *Nucl. Phys.*, vol. A354, nos. 1, 2, Feb. 23, 1981, pp. 535c–553c.
42. Sparrow, D. A.; Sternheim, Morton M.; and Silbar, Richard R.: Semiclassical Model for Pion Production by Neutrons on Nuclei. *Phys. Rev. C.*, Third ser., vol. 10, no. 6, Dec. 1974, pp. 2215–2220.
43. Yoo, K.-B.; and Landau, R. H.: Pion Annihilation in Nuclei, Spin, Isospin and Energy Dependence. *5th High Energy Heavy Ion Study—Proceedings,* LBL-12652 (UC-34, CONF-8105104) (Contract W-7405-ENG-48), 1981, pp. 736–737.
44. Ashery, Daniel: Pion Nucleus Reactions. *Nucl. Phys.*, vol. A354, nos. 1, 2, Feb. 23, 1981, pp. 555c–576c.

Symbols

c	speed of light (3×10^8 m/sec)
c.m.	center of mass
E	energy
E_π	pion total energy in projectile reference frame, MeV or GeV
f^2	unrationalized coupling constant (0.08), dimensionless
$f^2(\mathbf{k}_{\beta_\pi})$	form factor (defined in eq. (48) of ref. 26)
$F^2(\mathbf{k}_{\beta_\pi})$	form factor (defined in eq. (39) of ref. 26)
m_N	nucleon rest mass, MeV/c^2
m_Δ	isobar rest mass, MeV/c^2
m_π	pion rest mass, MeV/c^2
N	nucleon
p	momentum
p_β	nucleon momentum following isobar decay, MeV/c
p_π	pion momentum following isobar decay, MeV/c
T_N	nucleon kinetic energy, MeV
T_π	pion kinetic energy, MeV
Γ_{abs}	pion absorption effect width, MeV
Γ_{free}	free-state isobar resonance width (115 MeV)
Γ_Δ	isobar resonance width, MeV
Δ	isobar
Θ	pion angle of detection
λ	Pauli blocking factor, dimensionless
π^0	neutral pion
π^+	positively charged pion
π^-	negatively charged pion
σ	total cross section
σ_{nn}	neutron-neutron total cross section, mb
σ_{pn}	proton-neutron total cross section, mb
σ_{pp}	proton-proton total cross section, mb
$\sigma(X-Y)$	π^0 production cross section for collision involving nuclear species X and Y, mb or nb
$\sigma_{\Delta T}(\omega_\Delta)$	isobar formation cross section, mb or nb
$\frac{d^3\sigma\left(\pi_{\tau_f}\right)}{c^3\, d^3p_\pi/E_\pi}$	pion production Lorentz-invariant differential cross section, mb-GeV^{-2} or mb-MeV^{-2}
τ_f	final angular momentum
Ω	solid angle

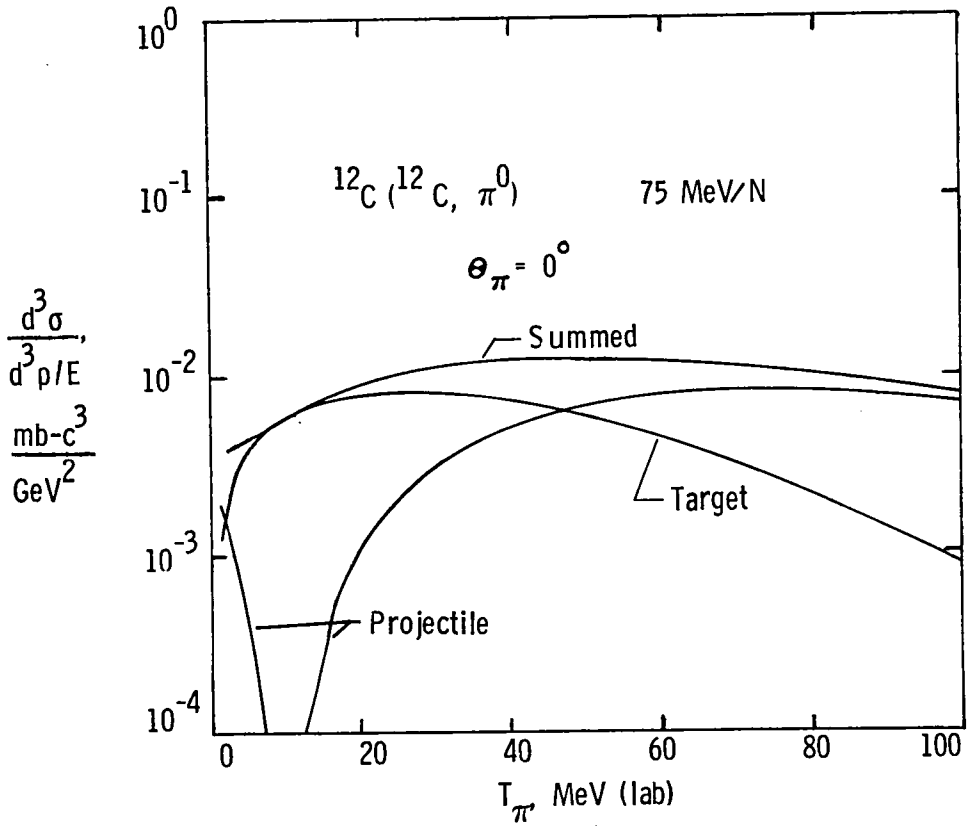

Figure 1. Theoretical Lorentz-invariant cross sections for π^0 production at $\Theta_\pi = 0°$ in carbon-carbon collisions at 75 MeV/N. Theoretical curves show decomposition of summed cross section in terms of contributions of pions from projectile and target.

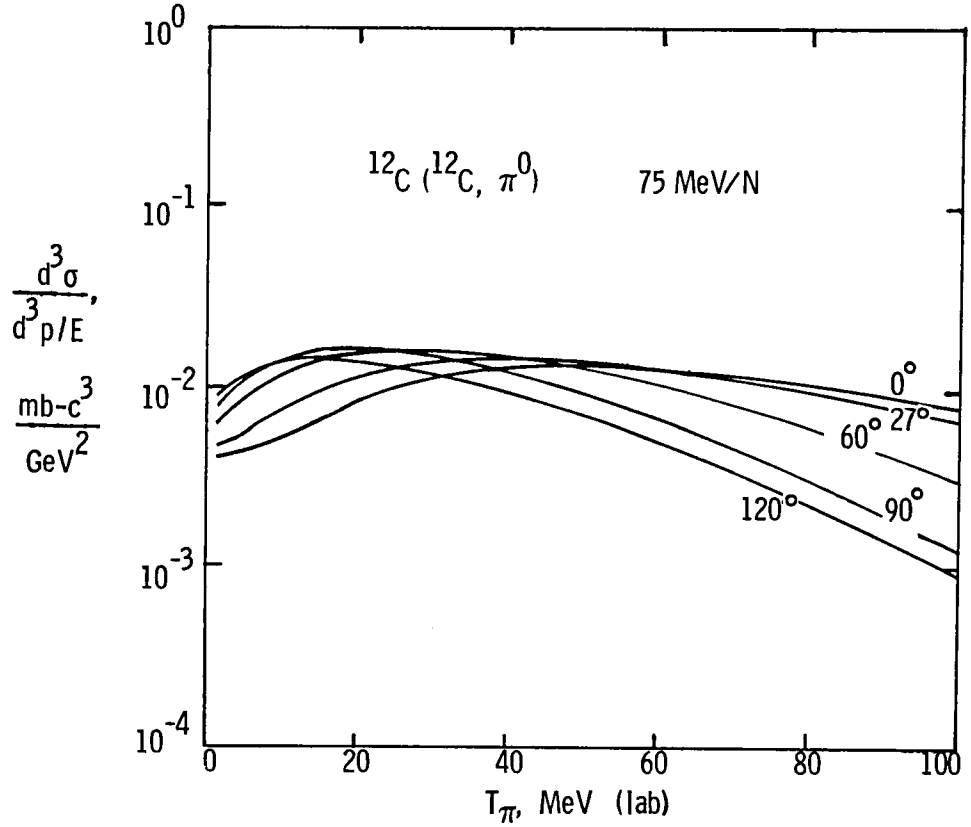

Figure 2. Theoretical Lorentz-invariant doubly differential cross sections for π^0 production at 75 MeV/N. Angular values are Θ_π.

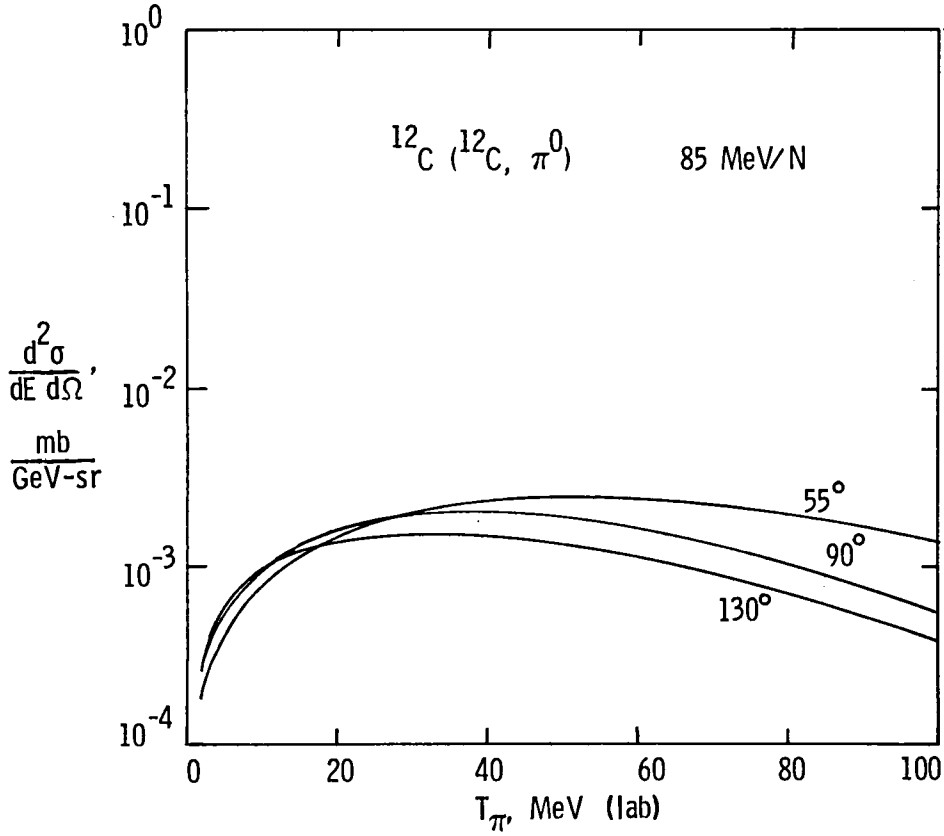

Figure 3. Theoretical noninvariant doubly differential cross sections for π^0 production at 85 MeV/N. Angular values are Θ_π.

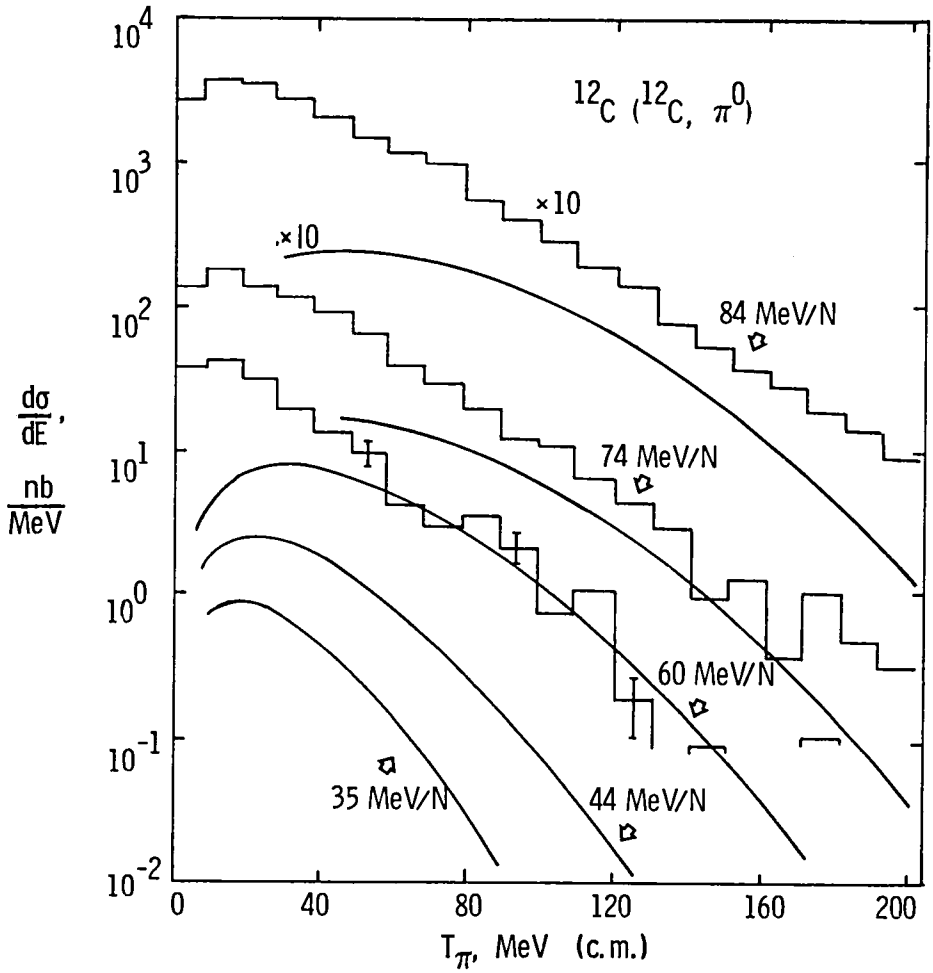

Figure 4. Spectral distributions for π^0 production. Solid curves display theoretical predictions of this study; histograms show experimental data of reference 7.

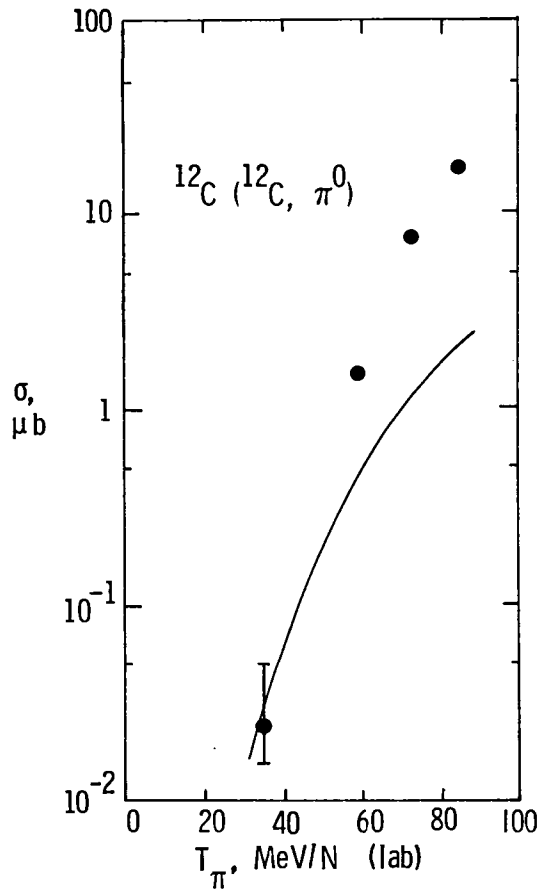

Figure 5. Total π^0 production cross sections as a function of incident projectile energy. Curve displays theoretical predictions; circles are experimental data of references 1 and 7.

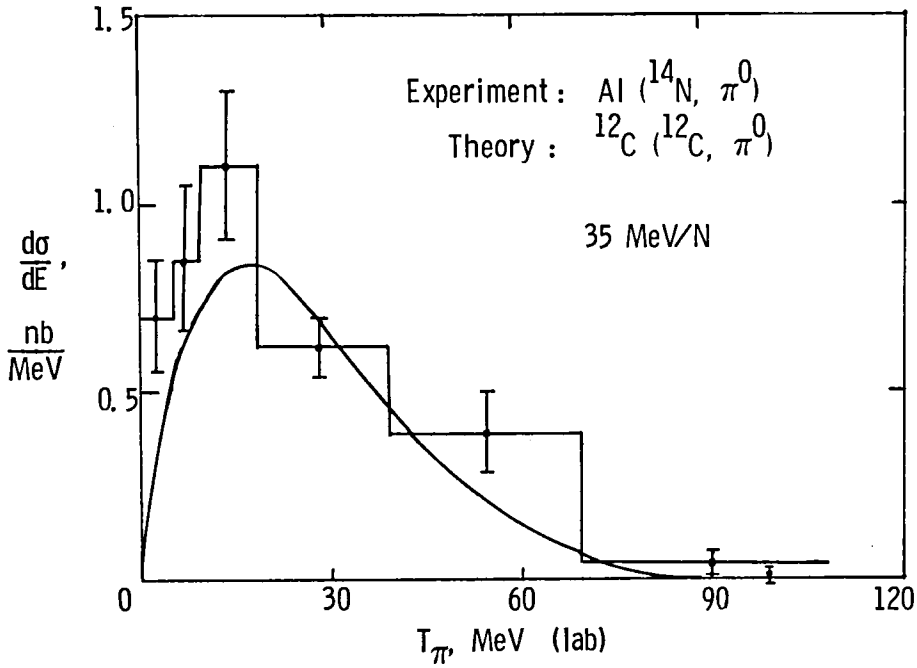

Figure 6. Spectral distributions for π^0 production. Solid curve displays theoretical predictions of this study for ^{12}C on ^{12}C; histogram and error bars display experimental data of reference 1 for Al on ^{14}N.

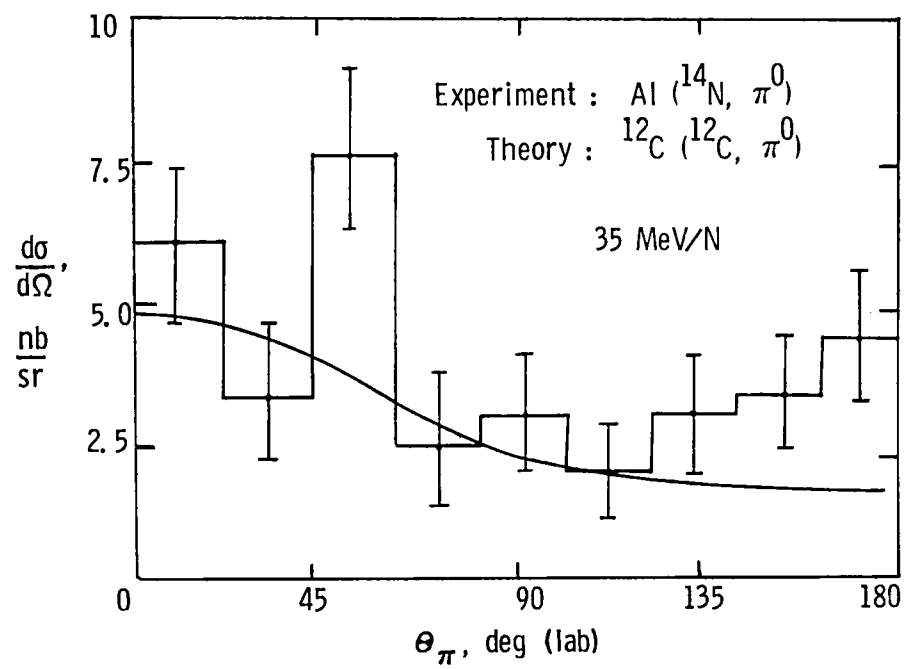

Figure 7. Angular distributions for π^0 production. Solid curve displays theoretical predictions of this study for ^{12}C on ^{12}C; histograms and error bars display experimental data of reference 1 for Al on ^{14}N.

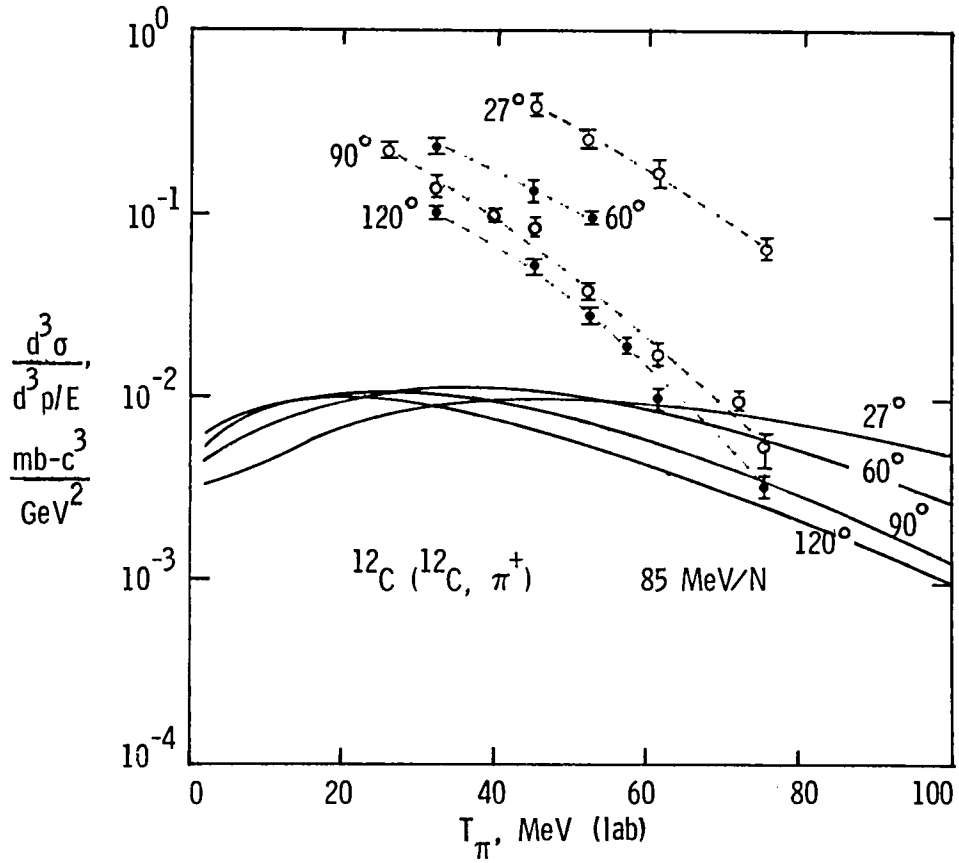

Figure 8. Theoretical and experimental (refs. 5 and 34) Lorentz-invariant doubly differential cross sections for π^+ production at 85 MeV/N. Solid lines represent theoretical predictions; dashed lines are drawn through experimental data points only to facilitate visual inspection; angular values are Θ_π.

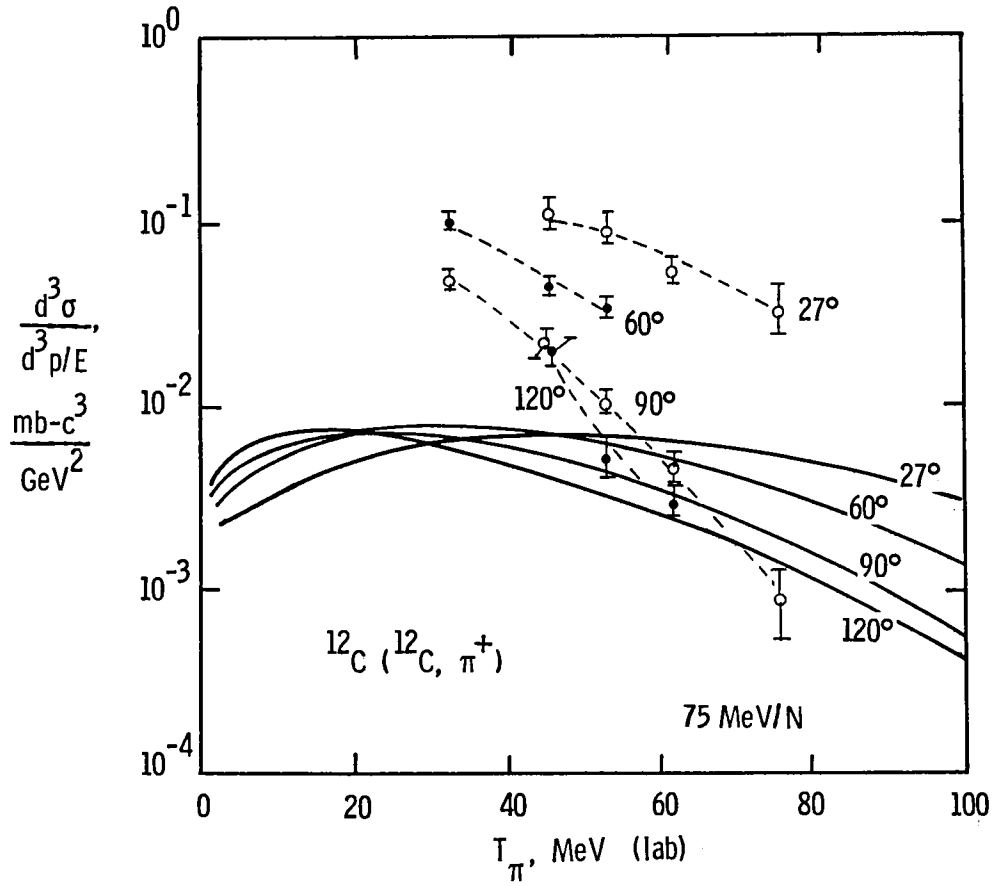

Figure 9. Theoretical and experimental (ref. 34) Lorentz-invariant doubly differential cross sections for π^+ production at 75 MeV/N. Solid lines represent theoretical predictions; dashed lines are drawn through experimental data points only to facilitate visual inspection; angular values are Θ_π.

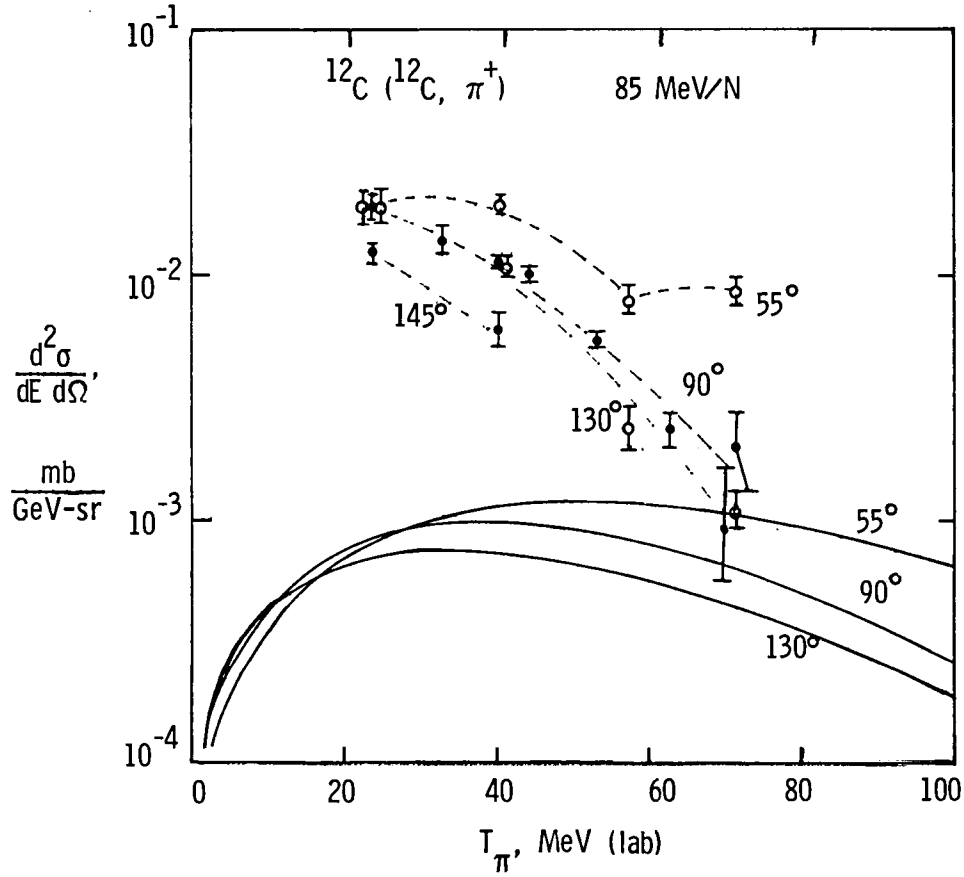

Figure 10. Theoretical and experimental (refs. 5 and 35) noninvariant doubly differential cross sections for π^+ production at 85 MeV/N. Solid lines represent theoretical predictions; dashed lines are drawn through experimental data points only to facilitate visual inspection; angular values are Θ_π.

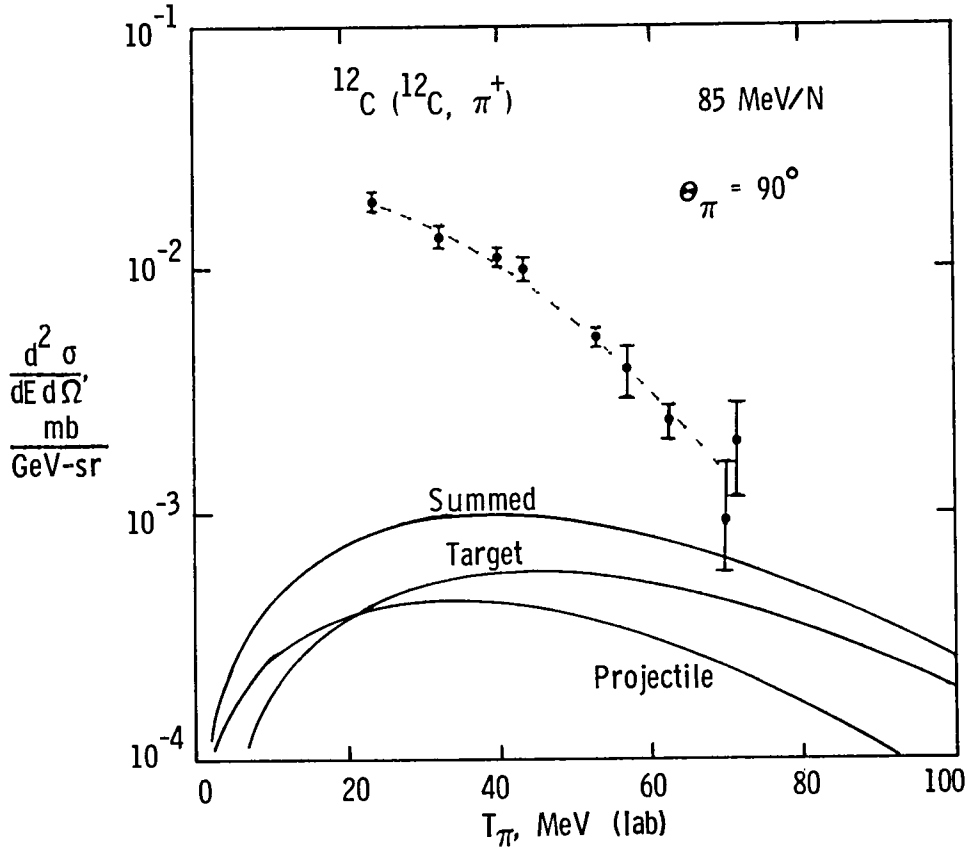

Figure 11. Theoretical and experimental (refs. 5 and 35) noninvariant doubly differential cross sections for π^+ production at 85 MeV/N for $\Theta_\pi = 90°$. Theoretical curves (solid lines) show decomposition of summed cross section in terms of contributions of pions from projectile and target.

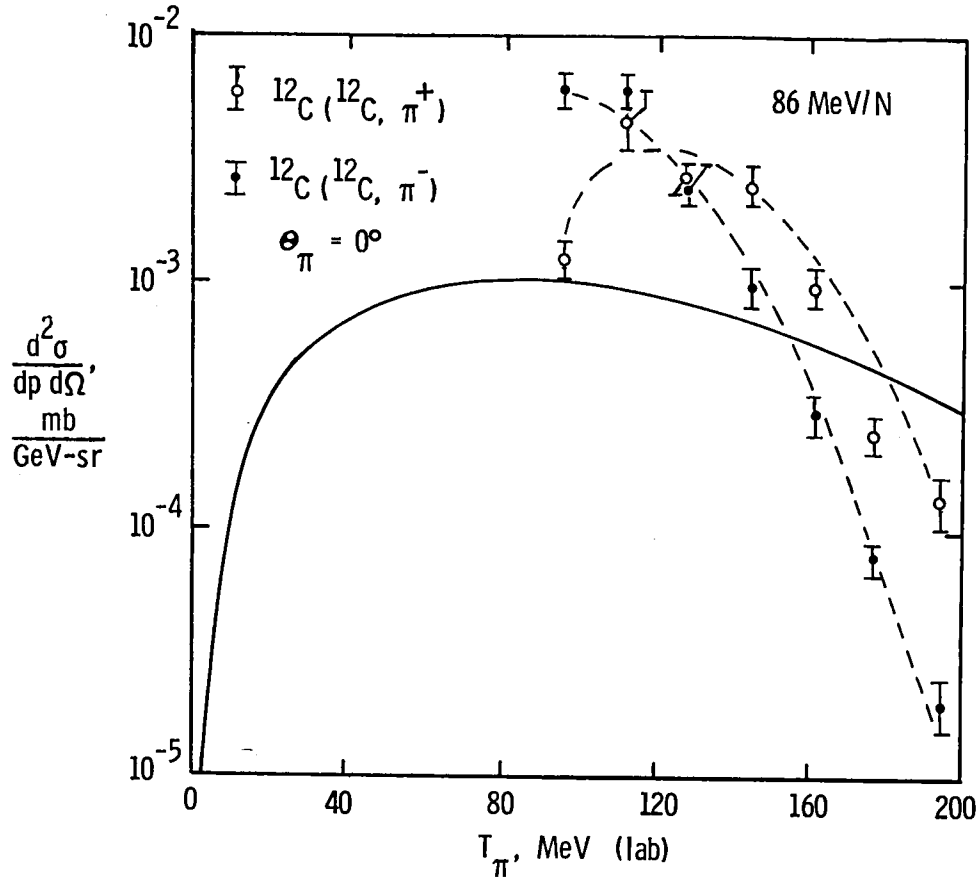

Figure 12. Theoretical and experimental (ref. 39) noninvariant doubly differential cross sections for π^+ and π^- production at 86 MeV/N. Solid line displays theoretical predictions; dashed lines are drawn through experimental data points only to facilitate visual inspection.

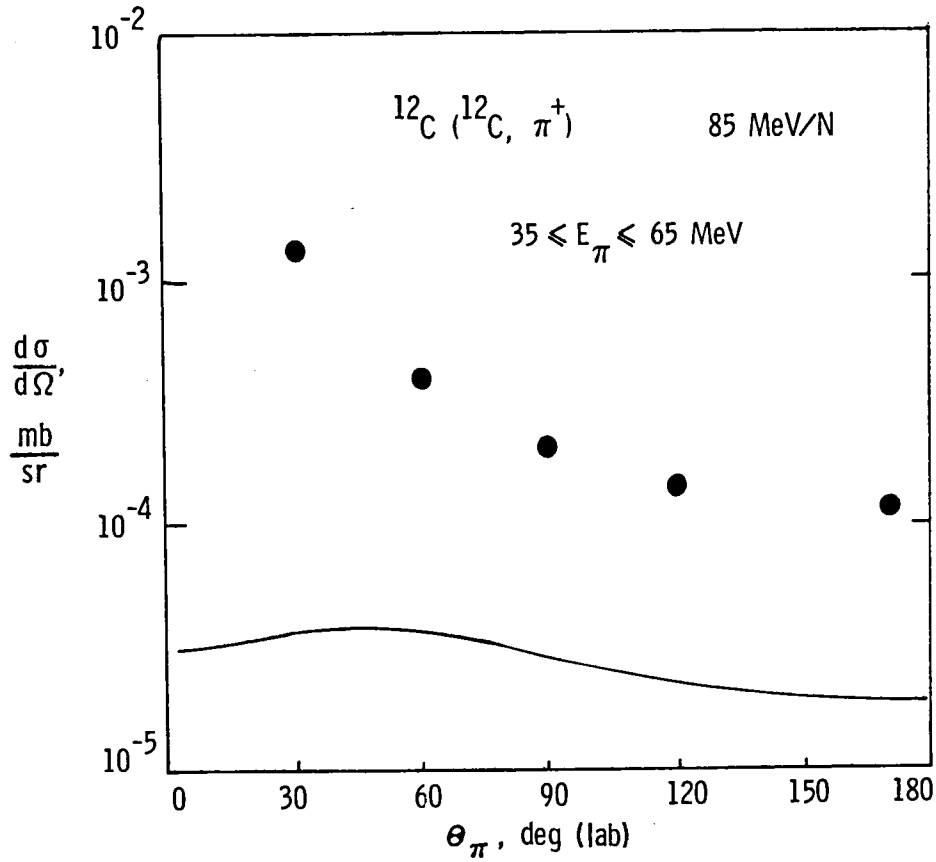

Figure 13. Theoretical and experimental (ref. 34) angular distributions for π^+ production at 85 MeV/N. Curve displays theoretical predictions; circles are experimental data points.

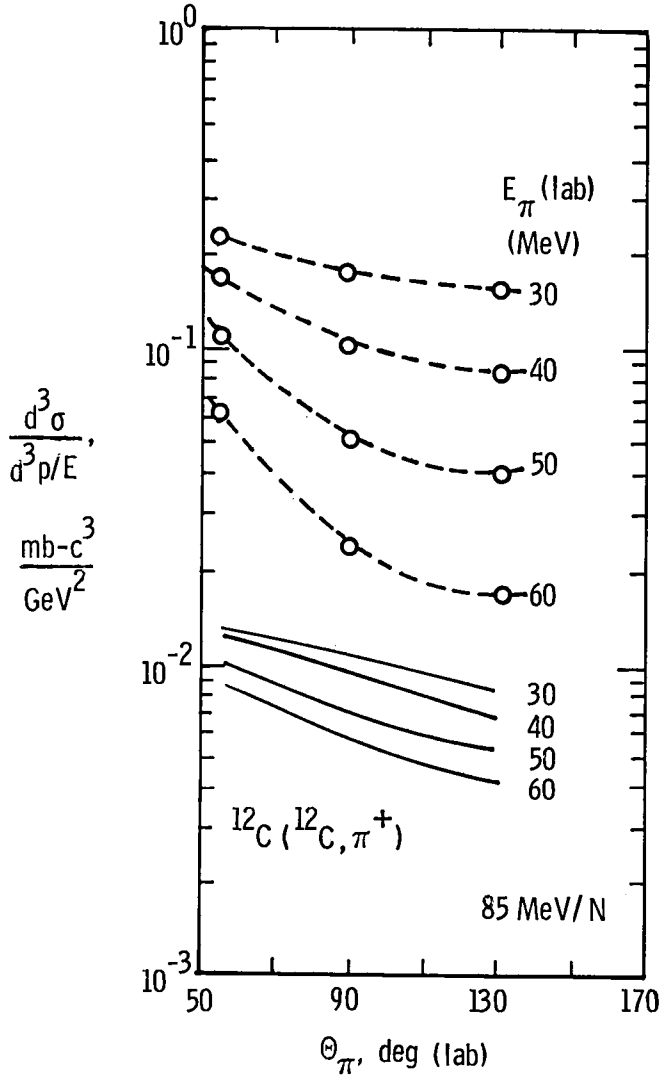

Figure 14. Theoretical and experimental (ref. 5) Lorentz-invariant doubly differential cross sections for π^+ production at 85 MeV/N. Circles and dashed lines represent experimental data; solid lines represent theoretical results; angular values are Θ_π.

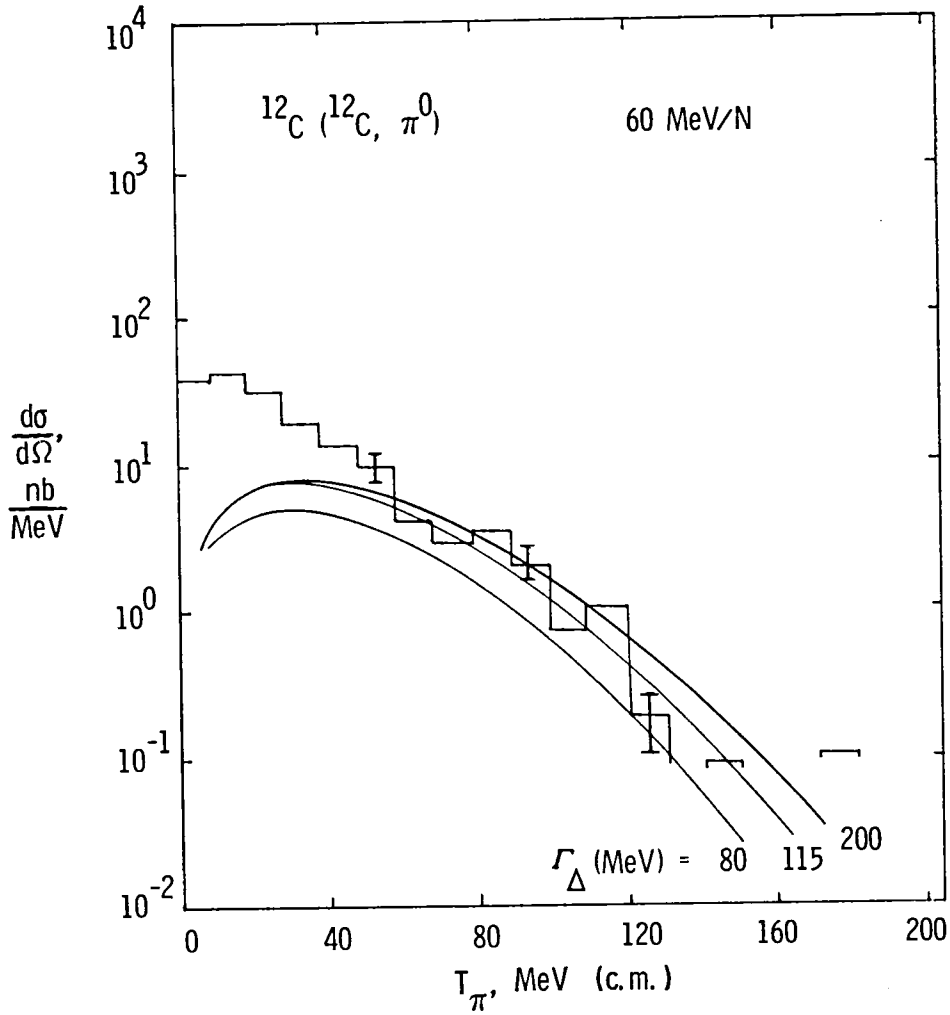

Figure 15. Spectral distributions for π^0 production at 60 MeV/N for isobar widths of 80, 115, and 200 MeV. Curves show theoretical predictions of this study. Histograms show experimental data from reference 7.

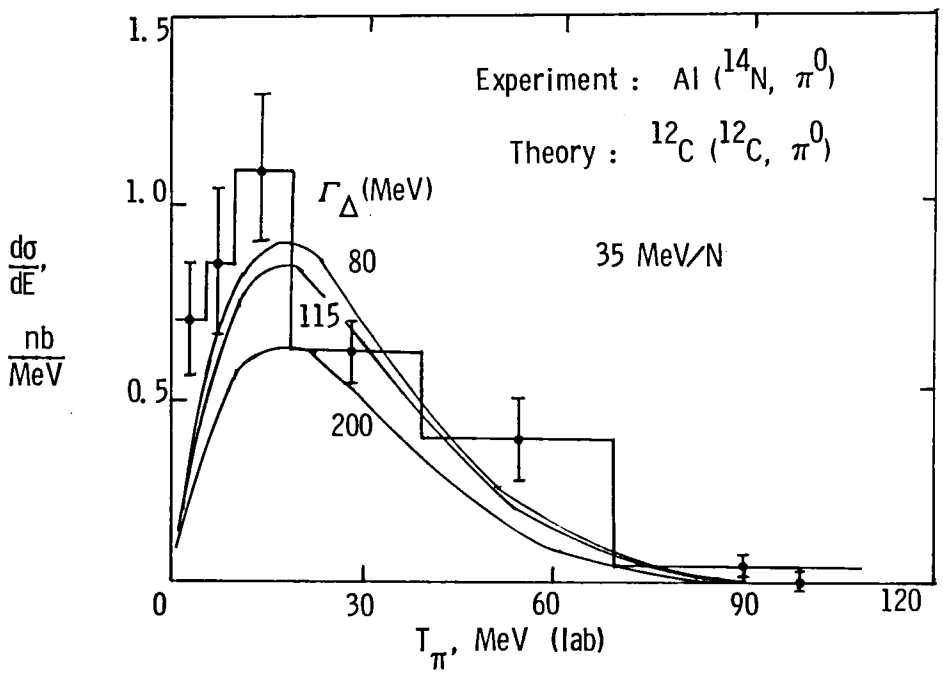

Figure 16. Spectral distributions for π^0 production at 35 MeV/N for isobar widths of 80, 115, and 200 MeV. Curves show theoretical predictions of this study for ^{12}C on ^{12}C. Histograms and error bars show experimental data from reference 1 for Al on ^{14}N.

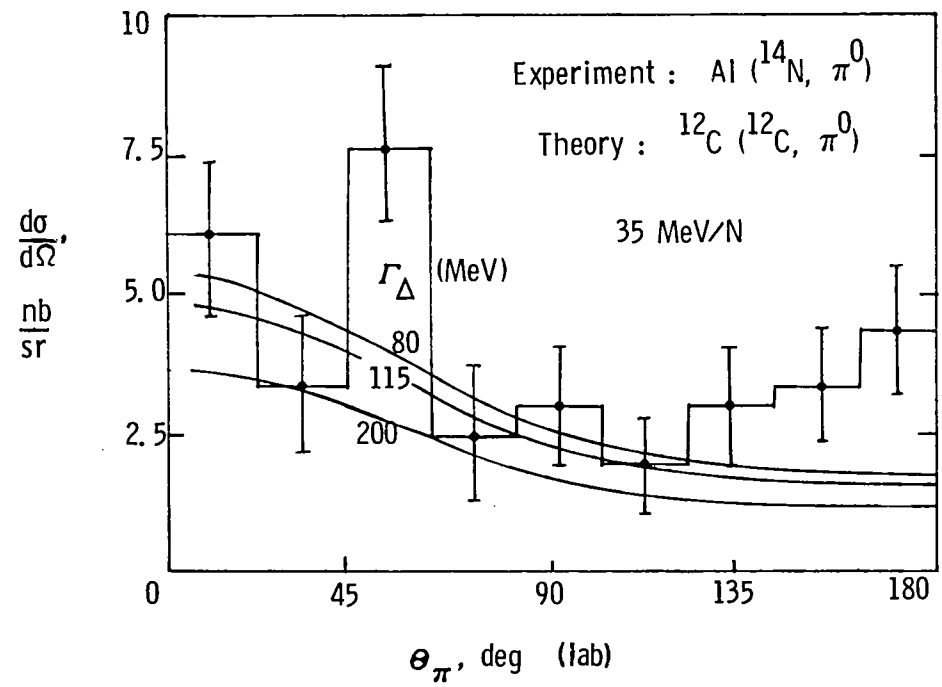

Figure 17. Angular distributions for π^0 production at 35 MeV/N for isobar widths of 80, 115, and 200 MeV. Curves show theoretical predictions of this study for ^{12}C on ^{12}C. Histograms and error bars show experimental data from reference 1 for Al on ^{14}N.

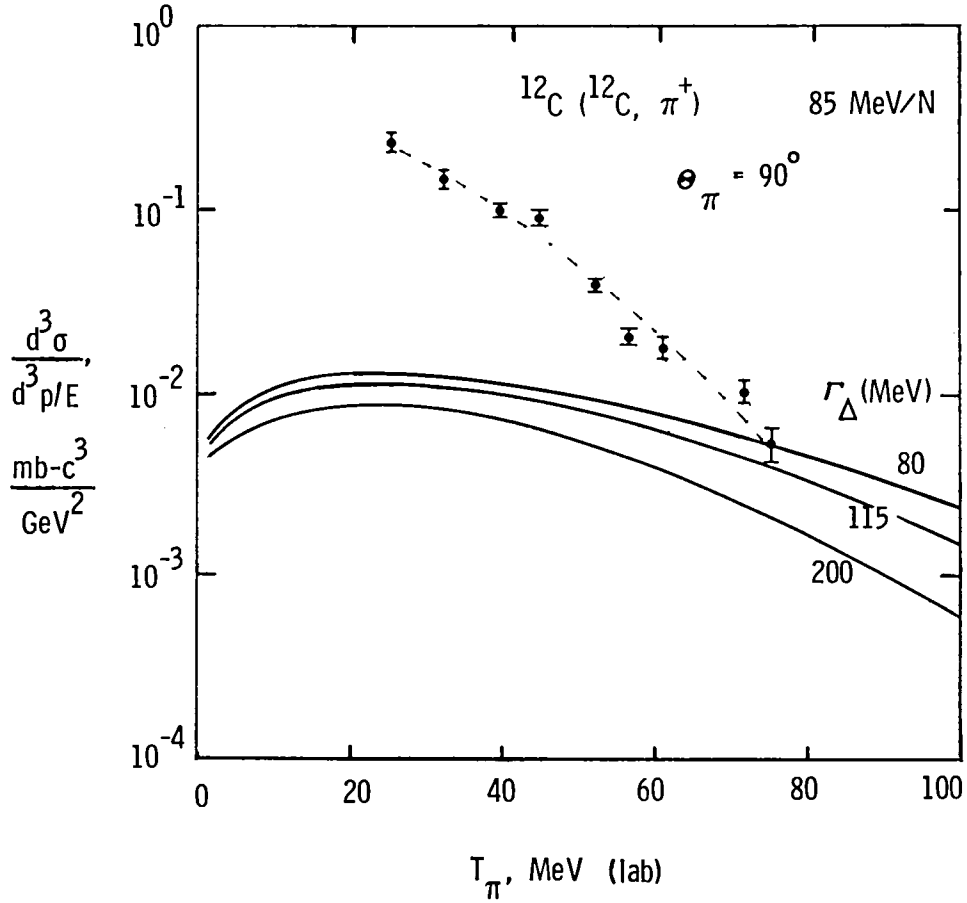

Figure 18. Theoretical and experimental (refs. 5 and 34) Lorentz-invariant doubly differential cross sections for π^+ production at 85 MeV/N at $\Theta_\pi = 90°$ for isobar widths of 80, 115, and 200 MeV. Solid lines are theoretical predictions; dashed line is drawn through experimental data points only to facilitate visual inspection.

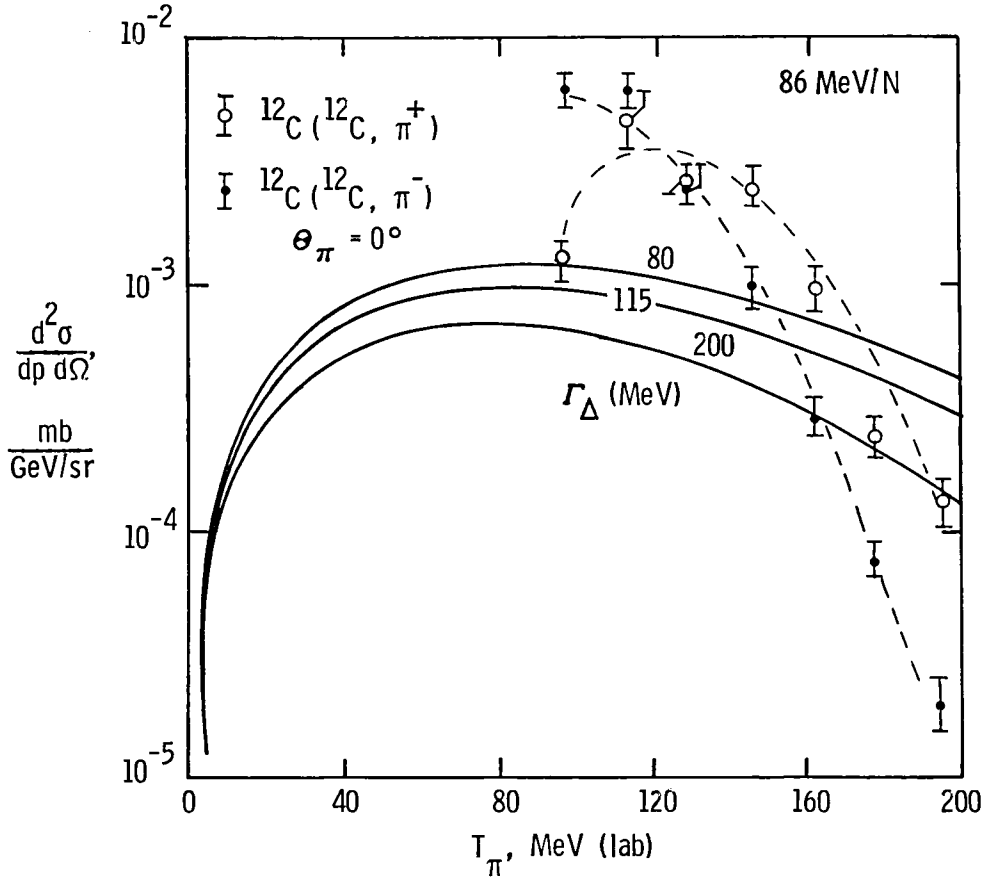

Figure 19. Theoretical and experimental (ref. 39) noninvariant doubly differential cross sections for π^+ and π^- production at 86 MeV/N for isobar widths of 80, 115, and 200 MeV. Solid lines are theoretical predictions; dashed lines are drawn through experimental data points only to facilitate visual inspection.

Standard Bibliographic Page

1. Report No.	2. Government Accession No.	3. Recipient's Catalog No.
NASA TP-2600		

4. Title and Subtitle	5. Report Date
Cross Section Calculations for Subthreshold Pion Production in Peripheral Heavy-Ion Collisions	August 1986
	6. Performing Organization Code: 199-22-76-01
7. Author(s): John W. Norbury, Francis A. Cucinotta, Philip A. Deutchman, and Lawrence W. Townsend	8. Performing Organization Report No.: L-16129
9. Performing Organization Name and Address: NASA Langley Research Center, Hampton, VA 23665-5225	10. Work Unit No.
	11. Contract or Grant No.
12. Sponsoring Agency Name and Address: National Aeronautics and Space Administration, Washington, DC 20546-0001	13. Type of Report and Period Covered: Technical Paper
	14. Sponsoring Agency Code

15. Supplementary Notes

John W. Norbury and Francis A. Cucinotta: Old Dominion University, Norfolk, Virginia.
Philip A. Deutchman: University of Idaho, Moscow, Idaho (supported by NSF grant no. PHY 8411009).
Lawrence W. Townsend: Langley Research Center, Hampton, Virginia.

16. Abstract

Total cross sections angular distributions, and spectral distributions for the exclusive production of charged and neutral subthreshold pions produced in peripheral nucleus-nucleus collisions are calculated by using a particle-hole formalism. The pions result from the formation and decay of an isobar giant resonance state formed in a ^{12}C nucleus. From considerations of angular momentum conservation and for the sake of providing a unique experimental signature, the other nucleus, chosen for this work to be ^{12}C also, is assumed to be excited to one of its isovector (1^+) giant resonance states. The effects of nucleon recoil by the pion emission are included, and Pauli blocking and pion absorption effects are studied by varying the isobar width. Detailed comparisons with experimental subthreshold pion data for incident energies between 35 and 86 MeV/nucleon are made.

17. Key Words (Suggested by Authors(s))	18. Distribution Statement
Subthreshold pions Spectral distributions Angular distributions Nucleus-nucleus collisions	Unclassified—Unlimited Subject Category 73

19. Security Classif.(of this report)	20. Security Classif.(of this page)	21. No. of Pages	22. Price
Unclassified	Unclassified	25	A02

For sale by the National Technical Information Service, Springfield, Virginia 22161

NASA-Langley, 1986

National Aeronautics and
Space Administration
Code NIT-4

Washington, D.C.
20546-0001